Supporting Information

Manipulating the Structure and Oxygen Evolution Reaction Performance in Metal Organic Frameworks via Symmetrical Control on the Functional Groups of Ligands

Zhi Li,[a] Yanan Li,[*a] Jie Lei,[a] Chengjie Yin,[a] XiaoHui Wu,[b] and Jinsong Hu[*a]

a. School of Chemical Engineering and Blasting, Anhui Province Engineering Technology Research Center of Coal Resources Comprehensive Utilization, Anhui Province Key Laboratory of Specialty Polymers, Anhui University of Science and Technology, Huainan 232001, China.

b. Henan Key Laboratory of Rare Earth Functional Materials, Zhoukou Normal University, Zhoukou, 466001, China.

EXPERIMENTAL SECTION

Preparation of Ni-BDC

Firstly, 0.18 mmol $Ni(CH_3COO)_2 \cdot 4H_2O$ (44.7 mg) were dissolved into 10 mL deionized water r (named A solution) and 0.75 mmol terephthalic acid (124.5 mg) were dissolved into 40 mL *N,N*-dimethylformamide (named B solution). B solutions is then quickly poured into A solutions under ultrasound at room temperature. Then, the solution was transferred into a 100 mL Teflon-lined stainless-steel vessel and sealed. After the solvothermal reaction for 24 h at 120 °C, the greenish-brown products were filtrated out and washed with *N,N*-dimethylformamide three times, and then dried in a vacuum at 50 °C overnight.

Preparation of Ni-BDC-1Br

Firstly, 0.18 mmol $Ni(CH_3COO)_2 \cdot 4H_2O$ (44.7 mg) were dissolved into 10 mL deionized water r (named A solution) and 0.75 mmol 2-bromoterephthalic acid (182.9 mg) were dissolved into 40 mL *N,N*-dimethylformamide (named B solution). B solutions is then quickly poured into A solutions under ultrasound at room temperature. Then, the solution was transferred into a 100 mL Teflon-lined stainless-steel vessel and sealed. After the solvothermal reaction for 24 h at 120 °C, the greenish-brown products were centrifugated and washed with *N,N*-dimethylformamide three times, and then dried in a vacuum at 50 °C overnight.

Preparation of Ni-BDC-4Br

Firstly, 0.18 mmol $Ni(CH_3COO)_2 \cdot 4H_2O$ (44.7 mg) were dissolved into 10 mL deionized water r (named A solution) and 0.75 mmol 2,3,5,6-tetrabromoterephthalic acid (358.3 mg) were dissolved into 40 mL *N,N*-dimethylformamide (named B solution). B solutions is then quickly poured into A solutions under ultrasound at room temperature. Then, the solution was transferred into a 100 mL Teflon-lined stainless-steel vessel and sealed. After the solvothermal reaction for 24 h at 120 °C, the greenish-brown products were filtrated out and washed with *N,N*-dimethylformamide three times, and then dried in a vacuum at 50 °C overnight.

Characterizations of Material

The pristine MOFs were characterized by X-ray diffraction (XRD, Bruker D8 ADVANCE X-ray diffractometer with Cu Kα radiation, 40 kV, 40 mA). Fourier transform infrared (FT-IR; Nicolet 6700) was used to find the functional groups. The surface morphologies and compositions of the investigated materials were observed by scanning electron microscopy (SEM; FEI Nova Nano SEM 450). Moreover, energy-dispersive X-ray spectroscopy (EDS) was used to analyze their elemental distribution. An X-ray photoelectron spectrometer (XPS, ESCALAB 250XI, Thermo Fisher, U.K.) were used to investigate the functional groups and surface oxidation states of products.

Electrochemical Measurements

The electrochemical performances of pristine MOFs based sheet-like electrodes were characterized on CHI760D electrochemical workstation. The as-prepared catalysts (1 cm × 1 cm) were used as working electrodes, a platinum foil (for OER)

was taken as the counter electrode, and an Hg/HgO reference electrode were employed to complete the three-electrode system. For the measurements, 1 M KOH electrolyte (pH = 13.88) was selected. The measured potentials were converted to the values based on the reversible hydrogen electrode (RHE) (ERHE=EHg/HgO + 0.098 + 0.0591pH), where EHg/HgO is the applied potential versus the value of Hg/HgO reference electrode. Due to the involved solution resistances, all the LSV polarization curves need to be adjusted by iR-correct. the reported current densities were calculated according to the geometric area of the pristine MOFs based sheetlike electrodes. The overpotential (η) was calculated by the following equations: ηOER = ERHE-1.23 V. The working electrode was conditioned by cycling thirty times with a scan rate of 100 mV/s prior to electrochemical measurements, the potential range is 0 to 0.8 V (for OER) vs. Hg/HgO. The polarization curves for the OER were recorded using a linear potential sweep with the rate of 2 mV/s. The electrochemical impedance spectroscopy (EIS) was measured in the same set up from 105 to 0.01 Hz with an AC amplitude of 5 mV. Long-term stability test was carried out using chronopotentiometric measurements. To evaluate the electrochemical active surface areas (ECSA) of the synthesized catalyst, the double-layer charging curves were tested using cyclic voltammetry at various scan rates. For the calculation of turnover frequency (TOF), the reductive negative scan peak area was firstly determined from cyclic voltammograms recorded at a specific scan rate, for example 300 mV/s. Charge (Q) can be obtained with the formula: Q = peak area/300 mV/s. Assuming a one-electron transfer process for both reduction and oxidation, the number of surface active sites (n) can be calculated with the equation: $n = Q/(1\times1.602\times10^{-19})$. TOF values are obtained from $TOF = j\times N_A/(4\times n\times F)$ (j = Current density, N_A = Avogadro number, F = Faraday constant).

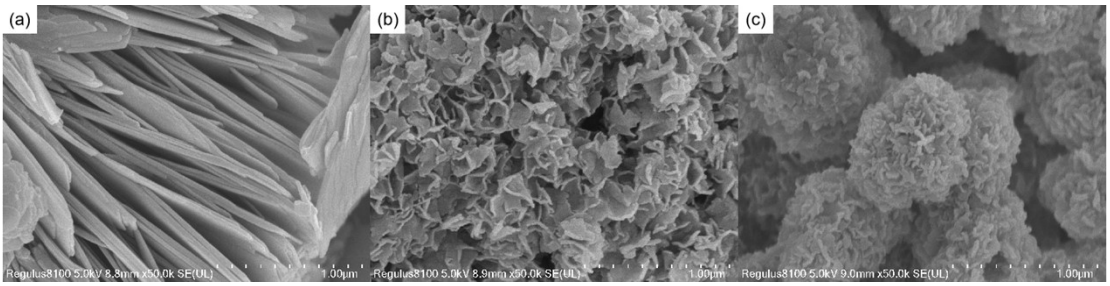

Figure S1. (a-c) SEM images of Ni-BDC, Ni-BDC-1Br and Ni-BDC-4Br.

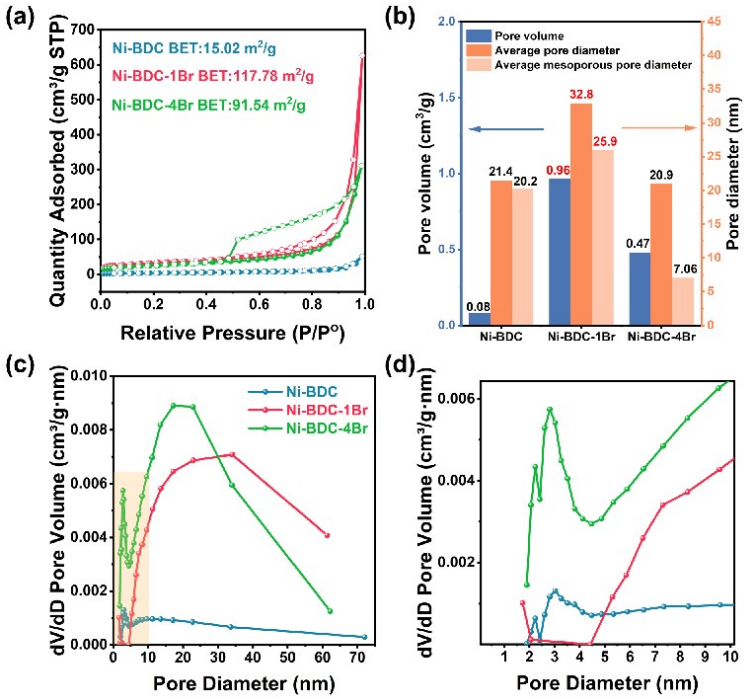

Figure S2. (a) N_2 adsorption/desorption isotherms of catalysts, (b) summary of pore volume and diameter, (c,d) pore size distribution.

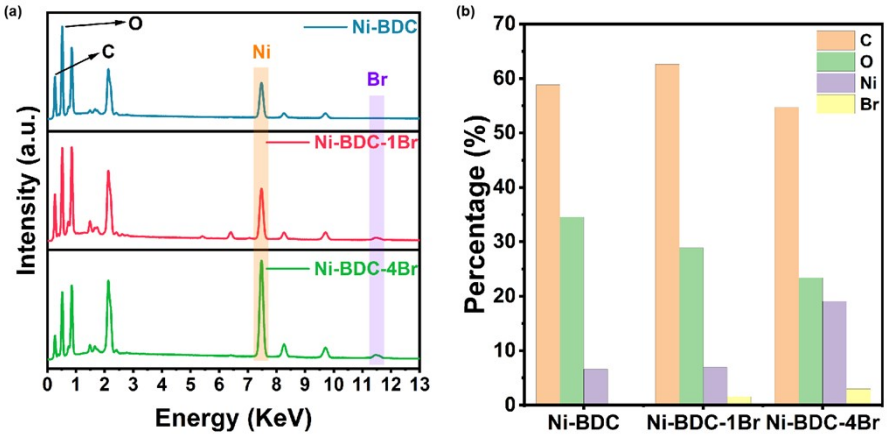

Figure S3. (a) Elemental spectra of catalysts, (b) The percentage of elements in catalysts.

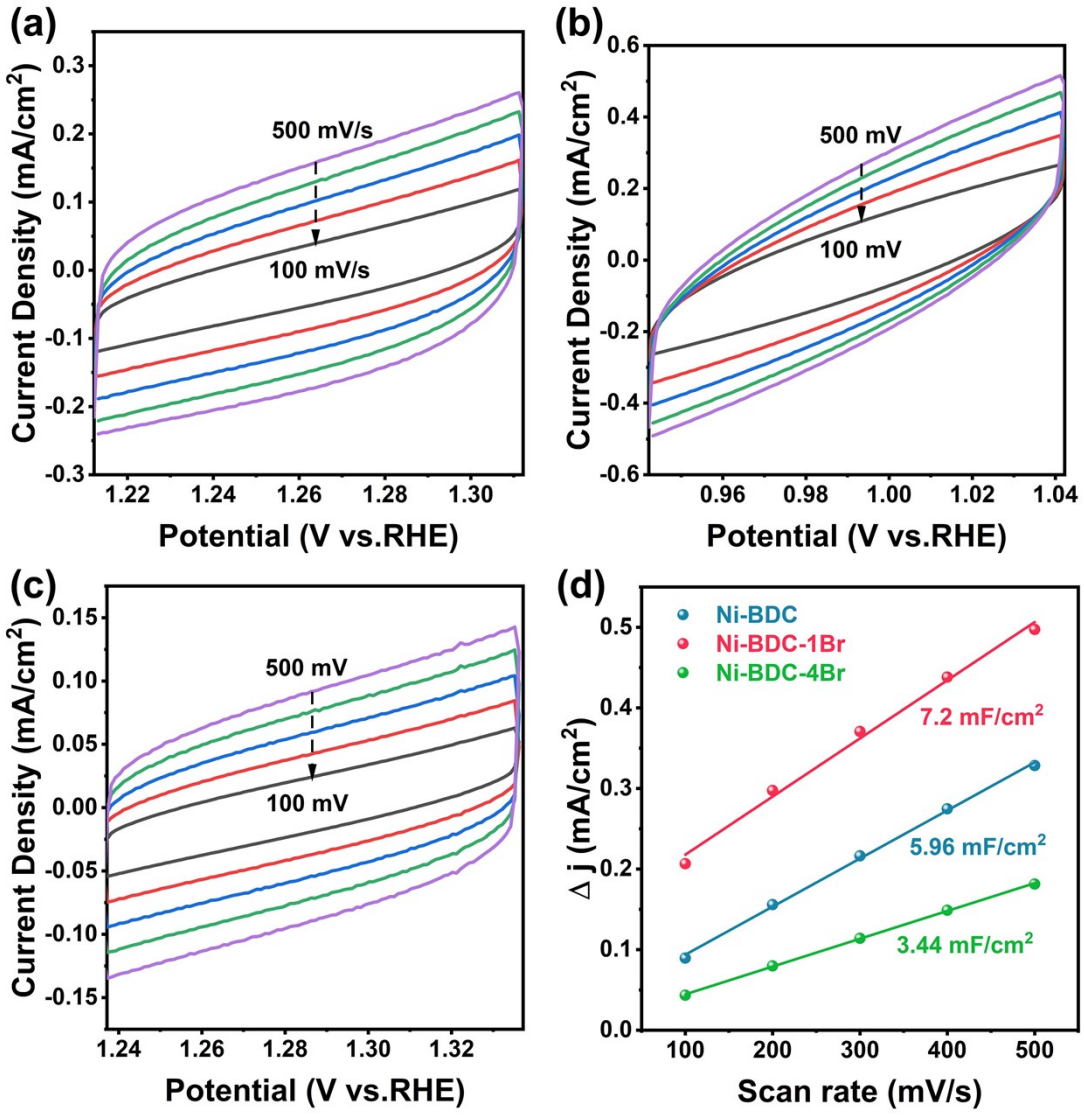

Figure S4 The scan-rate dependent CVs in the double-layer charging regions for (a) Ni-BDC, (b) Ni-BDC-1Br, (c) Ni-BDC-4Br, and (d) the calculated electrochemical double-layer capacitance.

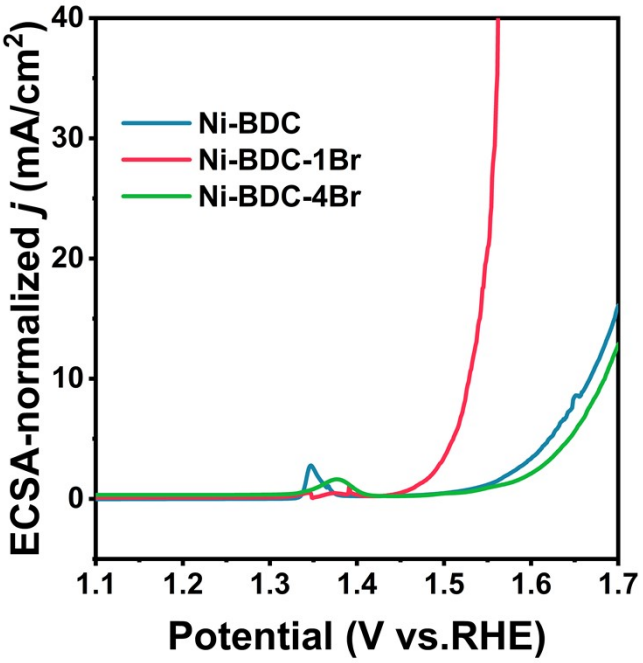

Figure S5. The LSV curve after ECSA normalization.

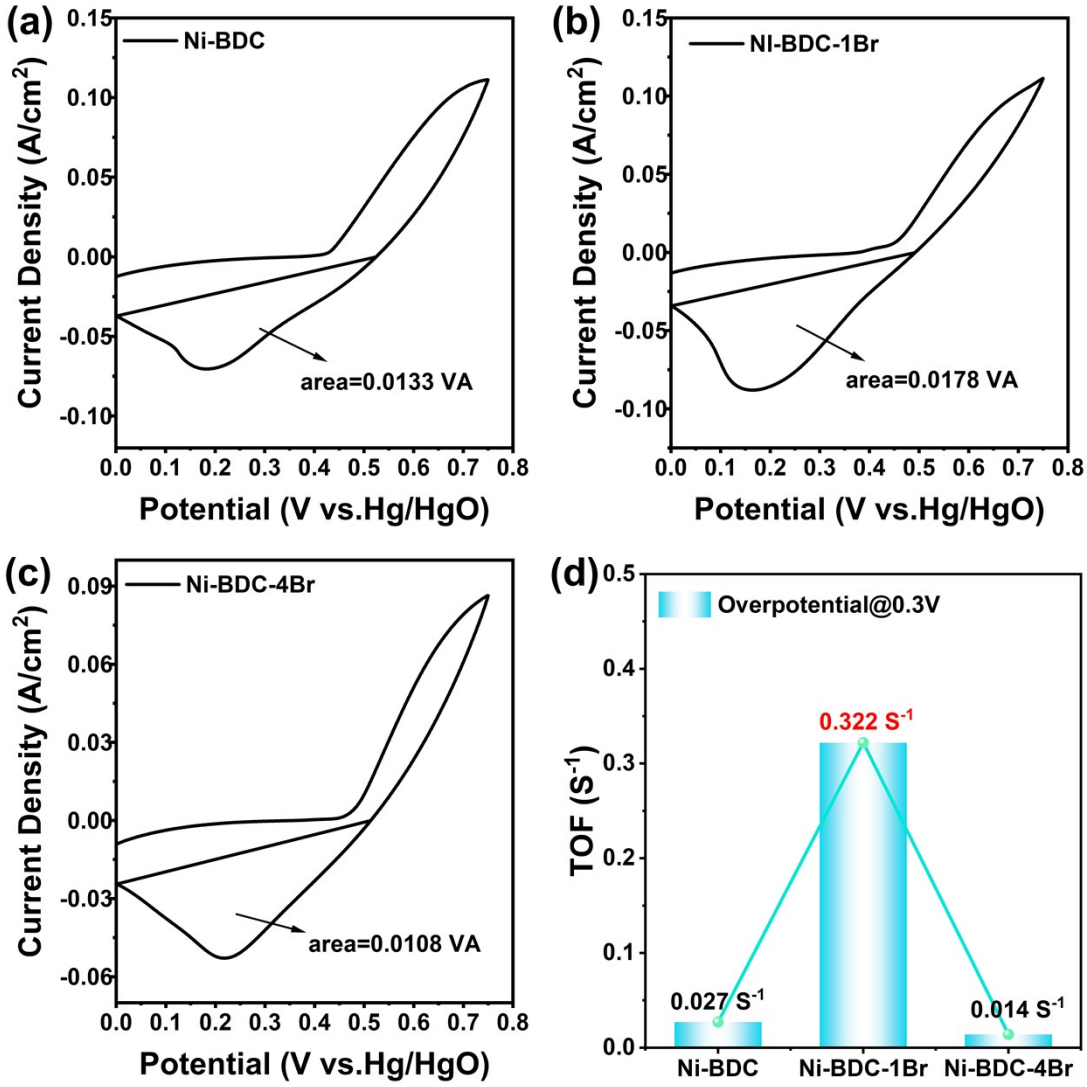

Figure S6 The CV measurement of (a) Ni-BDC, (b) Ni-BDC-1Br and (c) Ni-BDC-4Br for the determination of TOF. (d) Calculated TOF values at the overpotential at 0.3V.

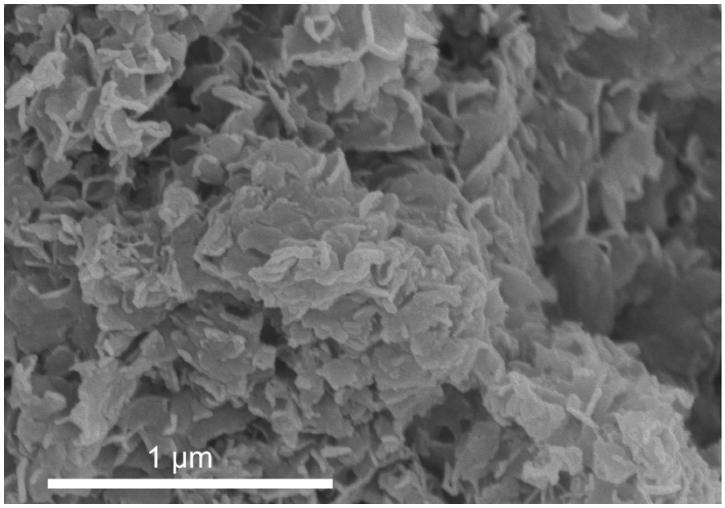

Figure S7 SEM image of the Ni-BDC-1Br sample covered on a graphite sheet electrode after the stability test.

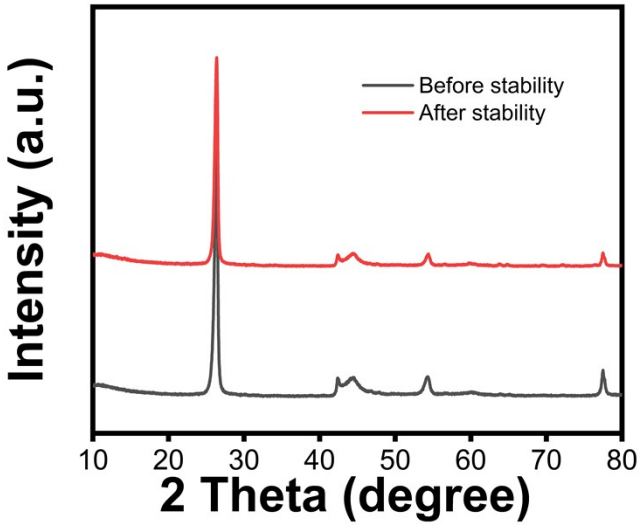

Figure S8 XRD patterns of the Ni-BDC-1Br sample covered on a graphite sheet electrode before and after the stability test.

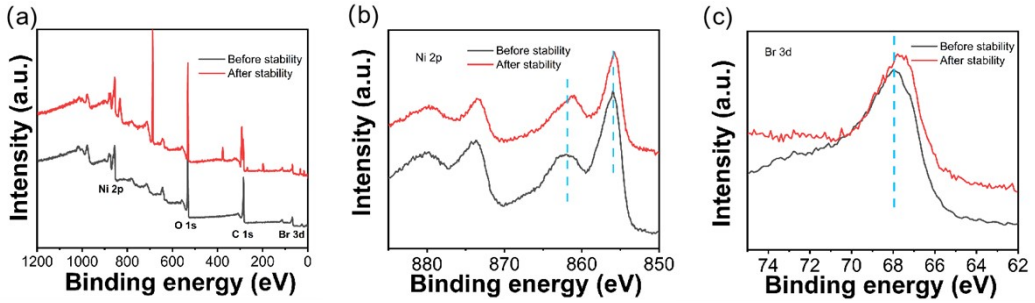

Figure S9 (a) XPS survey spectra, (b) High resolution Ni 2p and (c) High resolution Br 3d of the Ni-BDC-1Br sample covered on a graphite sheet electrode before and after the stability test.

Table 1. The OER performance comparison

catalysts	Overpotential (mV) @10 mA cm	Tafel solp (mV dec^{-1})	ref.
Ni-nitrodopamine (NDA/MWCNTs-a)	285	73	1
Ni@NCS-800	330	54	2
Br-Ni-MOF hollow prisms	306	79.1	3
Ni-MOF-A/CP	441	80	4
Ni-MOF@Fe-MOF	265	82	5
Ni-250-2@NF	289	95	6
NiMOF/BP-240	260	76	7
Ni-DA-MWCNTs-a	267	61	8
Ni-BDC-1Br	247	58	this work

References:

1. S. Kiran, G. Yasmeen, Z. Shafiq, A. Abbas, S. Manzoor, D. Hussain, R. A. Pashameah, E. Alzahrani, A. K. Alanazi, M. N. Ashiq, *Fuel*, 2023, **331**, 125881.

2. K. B. Patel, B. Parmar, K. Ravi, R. Patidar, J. C. Chaudhari, D. N. Srivastava, G. R. Bhadu, *Appl. Surf. Sci.*, 2023, **616,** 156499.

3. W. Cheng, S. Xi, Z. P. Wu, D. Luan, X. W. Lou, *Sci. Adv.,* 2021, **7**, eabk0919.

4. D. Yu, Z. Q. Jiang, J. Lu, Y. F. Li, W. J. Fan, H. Y. Yang, T. Wen, *Inorg. Chem.,* 2021, **60**, 1305–13095. 5. K. Rui, G. Q. Zhao, Y. P. Chen, Y. Lin, Q. Zhou, J. Y. Chen, J. X. Zhu, W. P. Sun, W. Huang, S. X. Dou, *Adv. Funct. Mater.,* 2018, **28,** 1801554.

6. S. M. Wang, Y. Zhang, X. Y. Deng, Z. Z. Ma, R. T. Cheng, Z. H. Wan, J. P. Li, X. G. Wang, *J. Mater. Chem. A,* 2023, **11**, 5222-5232.

7. W. F. Zhai, Y. Chen, Y. D. Liu, T. Sakthivel, Y. Y. Ma, Y. B. Qin, Y. Q. Qu, Z. F. Dai, *ACS Nano,* 2023, **17,** 17254–17264

8. S. Kiran, S. Houda, G. Yasmin, Z. Shafiq, A. Abbas, S. Manzoor, A. Syed, A. M. Elgorban, N. S. S. Zaghloul, M. N. Ashiq, *Energy Fuels,* 2023, **37**, 5388–5398